Proceedings of the 2005 IEEE
Engineering in Medicine and Biology 27th Annual Conference
Shanghai, China, September 1-4, 2005

Electrical Stimulation to Restore Vestibular Function – Development of a 3-D Vestibular Prosthesis

Charles C. Della Santina[12], Americo A. Migliaccio[1] and Amit H. Patel[2]
Departments of [1]Otolaryngology-Head & Neck Surgery and [2] Biomedical Engineering
Johns Hopkins School of Medicine, Baltimore, MD, USA

Abstract— **Patients who fail to compensate for bilateral loss of vestibular sensory function are disabled by disequilibrium and illusory movement of the visual field during head movement. An implantable prosthesis that restores vestibular sensation could significantly improve quality of life for these patients. To be effective, such a device should encode head rotation in all 3 dimensions. We describe the 3-dimensional angular vestibulo-ocular reflex of normal chinchillas and vestibular-deficient chinchillas undergoing functional electrical stimulation of the vestibular nerve. We also describe the design and fabrication of a head-mounted, 8 electrode vestibular prosthesis that encodes head movement in 3 dimensions.**

Keywords— **3D, vestibular prosthesis, balance, FES, labyrinth, semicircular canal, bilateral vestibular deficiency**

I. Introduction

During head rotations typical of daily life (as in walking or driving), the angular vestibulo-ocular reflex (aVOR) causes binocular eye rotations approximately equal to the opposite of head rotation, stabilizing gaze and maximizing visual acuity. In humans, it acts with high fidelity over the range of most natural head movements (~0.5-10 Hz) and can accurately track head movements faster than 300°/s and 5000°/s^2. It is the only oculomotor tracking system that works over this range, because both smooth pursuit and optokinetic nystagmus fail above ~1 Hz [1]. For patients with poorly compensated bilateral vestibular-deficiency due to ototoxic drugs, Ménière's disease, meningitis, genetic defects, or other insults to the inner ear, head movements in any direction significantly degrade visual acuity [2]. For these patients, an implantable neuroelectronic prosthesis that measures head rotation and selectively encodes it as spike trains on branches of the vestibular nerve could significantly improve quality of life.

Classic studies by Cohen, Suzuki and their colleagues qualitatively described the direction of nystagmus generated by single- and multi-electrode stimulation of vestibular nerve branches to the semicircular canals [3]. Coupled with studies of vestibular nerve afferent responses to galvanic stimuli [4]-[6], advances in miniaturization of rotational accelerometers, and experience gained from decades of cochlear implant development, these studies suggest that a head-mounted, implanted prosthesis for restoration of vestibular sensation and aVOR function should be feasible.

Gong and Merfeld described a 1-channel prototype of such a device [7],[8]. In otherwise normal guinea pigs and squirrel monkeys rendered unresponsive to head rotation by surgical plugging of semicircular canals, that device generated partly compensatory eye movements for head rotations about axis of rotational sensitivity of the device. The aVOR gain (–eye velocity / head velocity) observed was significantly less than that of the normal aVOR before canal plugging, suggesting that more intense stimuli or more optimal stimulus coupling to the vestibular nerve is needed.

Unfortunately, the three ampullary nerves (the terminal branches of the vestibular nerve, in the neuroepithelium of the ampullated region of each semicircular canal) and the vestibular nerve branches to otolith endorgans are all close to each other in small animals. Attempts to increase response amplitude by simply increasing stimulus intensity can fail due to inadequate selectivity of stimulation. Spurious stimulation of vestibular nerve branches other than the intended target leads to poor control of eye movement direction. Thus, increasing response gain and ensuring accurate encoding of head movement direction will likely require improvements in stimulation selectivity. Improving stimulus selectivity should be facilitated by measurement and analysis of eye movements in all 3 dimensions, so that effects of changes in electrode design and stimulus protocols can be accurately assessed.

We describe eye movement responses to head rotation and functional electrical stimulation using 3-dimensional oculography in chinchillas (*Chinchilla laniger*). Drawing on these findings, we have developed a prototype vestibular prosthesis that simultaneously encodes head rotations in all 3 dimensions, resolves them into canal-plane components, and presents them as pulse-frequency-encoded stimuli to the ampullary nerves innervating 3 or more semicircular canals.

II. Methods

A. Characterizing the 3-Dimensional VOR of Chinchillas Before and After Semicircular Canal Occlusion

Adult wild-type 450-650g chinchillas were used for all experiments, which were performed in accordance with a protocol approved by the Johns Hopkins Animal Care and Use Committee. To restrain animals for whole body rotation, head bolts were placed using dental acrylic under ketamine/xylazine anesthesia (at least 16 hours before testing) or sevoflurane. Sevoflurane was used to sedate animals during placement in the testing apparatus. Animals

Manuscript received May 2, 2005. This work was supported by the National Institute on Deafness and Other Communication Disorders (K08-DC006216 and R01-DC002390), by an American Otological Society Clinician-Scientist Award to CCDS, and by a Johns Hopkins School of Medicine Ross Clinician-Scientist Award to CCDS. Address correspondence to Charley C. Della Santina, PhD MD; Dept. of Otolaryngology – Head & Neck Surgery, 601 North Caroline St., Room JHOC 6253, Baltimore, MD 21287 voice: 410-955-7381; fax: 410-614-8610; e-mail: charley.dellasantina@jhu.edu

were tested fully alert (> 20 minutes after last sevoflurane).

Eye movements of 9 normal animals were recorded in darkness using a binocular, 3-D video-oculography (VOG) system described in detail elsewhere [9]. Fick rotation components were computed in real time from locations of 3 fiducials affixed to each cornea. VOG sample rate was limited to 30 samples/s, effectively limiting VOG tracking to ~2 Hz and below. (The same system has since been upgraded to a 130 frame/s sampling rate, while maintaining real-time 3-D eye rotation acquisition.)

Eye movements of the same normal animals were also recorded at 200 or 1000 samples/s using a 3-field magnetic scleral search coil system and an orthogonal pair of coils temporarily affixed to the cornea of each eye. This system has been described in detail elsewhere [9],[10].

Eye and head movements were analyzed using 3-dimensional rotational kinematics in a suite of software developed in our laboratory by one of the authors (AAM). Rotations are resolved into horizontal (yaw), left-anterior/right-posterior (LARP), and right-anterior/left-posterior (RALP) components along mutually orthogonal axes that approximate the axes of rotation of the semicircular canals.

In 4 animals, bilateral plugging of semicircular canals, disruption of the otolith endorgans, and implantation of wire electrodes near one or more semicircular canal cristae were performed at the time of head bolt placement. Monopolar electrodes were fashioned from 254 um diam Teflon-coated Ag wire (Ag10T, Sigmund Cohn Co., Mount Vernon, NY), stripped 0.3 mm. Bipolar electrodes were made of twisted pairs of 75 um diameter Pt/Ir wire (AS169-40, Cooner Wire, Chatsworth, CA) stripped 0.2 mm, with ~0.3 mm interelectrode spacing. A reference electrode (Ag10T wire stripped ~1 cm) was embedded in neck musculature. Electrical stimuli were delivered via one or more mono- or bipolar electrodes as pulse-frequency-modulated (typically 0-300 pulses/s) biphasic pulses of 20-200 μA/phase, 20-500 μs/phase, intrapulse interval 0-200 μs, modulated by measured head rotational velocity in real time.

For testing the VOR response to head rotation, animals were mounted on a digitally-controlled rotator able to deliver whole-body rotations at up to 5000°/s at DC-20 Hz about an Earth-vertical axis (130-80/ACT2000, Acutronic USA, Pittsburgh, PA). Mounted atop this rotator was a gimbaled stereotaxic frame that could be tilted to align the axis of any semicircular canal with the motor axis.

D. Design of a 3D Vestibular Prosthesis

We designed a prototype vestibular prosthesis to be able to simultaneously encode head rotations of ± ~0.2 to 450°/s in each of 3 dimensions and deliver pulse-frequency-modulated, biphasic, constant current stimuli via 8 electrodes. In brief, the device comprises a microcontroller that continually samples (at 100 samples/s) input from 3 mutually orthogonal micromachined gyro accelerometers and accordingly modulates the pulse frequency of stimuli on each electrode (or pair of electrodes). Electrodes can be configured post-implantation under software control as 4 isolated bipolar electrode pairs, 7 monopolar electrodes with a common reference, or a combination of bipolar and monopolar. The device can be reprogrammed *in situ* via a JTAG programming interface that allows full access to all registers and memory of the microcontroller. Designed to fit on the head of a chinchilla or other small mammal, the circuitry is implemented using surface mount technology and is ~30 mm x 30 mm x 11 mm; when packaged within a 35 mm x 35 mm x 15 mm plastic case, it weighs 19g (not counting an external battery). It can be rigidly connected to the head bolt already in place for stabilizing an experimental animal during head rotation experiments.

In the following sections, we describe the design and fabrication of this device in more detail.

a. Sensors – The device employs 3 micromachined gyro rotational accelerometers (ADXRS300, Analog Devices, Norwood, MA) oriented orthogonal to each other. Each encodes rotational velocity about a single axis, over a range of ± ~0.2 to 450°/s and bandwidth of DC-40 Hz. To reduce the computational load on the microcontroller, the device is affixed to the skull in an orientation that aligns the sensors with the planes of the implanted semicircular canals. The output of each sensor can then directly modulate the pulse frequency of the corresponding canal's stimulus channel, without the computational overhead of performing a 3 x 3 rotation matrix multiplication of the 3 x 1 input data vector.

b. Processor – An MSP430F149 microcontroller (Texas Instruments, Dallas, TX) controls the device. It is an ultra low-power microcontroller featuring a 16-bit RISC CPU, 2 KB of RAM and 60 KB of flash memory, two multifunction timers, an 8-channel 12-bit A/D converter, two universal serial synchronous/asynchronous communication interfaces (USARTs), a hardware multiplier, and 48 bidirectional I/O pins. The CPU and one set of timers are clocked by a 6 MHz crystal for timing biphasic stimulus pulses at sub-microsecond resolution; another set of timers is clocked by a 32,768 Hz crystal for encoding pulse-frequency modulation.

c. Current Source and Switching – A single current source (actually, a current sink) is shared by all output channels of the device. It is a single-supply voltage-to-current converter built around an op-amp (OPA2345, Texas Instruments) chosen for its low-power-consumption and adequately high slew rate (2 V/μs). The op amp output sets the gate voltage of a FET transistor as required to maintain a current of 2-512 μA through the electrodes, FET and a 3.01KOhm sense resistor. The current source's control voltage is set by one of the 3 channels of an 8 bit MAX 5101 D-A converter (Maxim, Sunnyvale, CA) under CPU control. This approach allows a user to set the stimulus current amplitude for each channel independently, and leaves available the option of using pulse-amplitude modulation or asymmetric biphasic pulses.

Each of the 8 electrode leads connects via a 1 μF blocking capacitor to one of the 8 normally open outputs of each of 2 MAX308 analog multiplexers (Maxim, Sunnyvale, CA).

The common pin of the "anode" MAX308 connects to a 24 V compliance voltage, while "cathode" MAX308 common terminal connects to the current sink. To generate biphasic current pulses up to ~230 μA through a 100 kΩ total electrode impedance via a pair of electrodes Z1 and Z2, the MSP430 addresses the MAX308's to alternately connect Z1 (initially the anode) to 24 V and Z2 (initially the cathode) to the current sink. At the end of the anodic-on-Z1 pulse, both electrodes are disconnected to create an intra-pulse interval. Connections are then swapped to make Z1 the cathode and Z2 the anode long enough to complete a charge-balanced biphasic pulse. This floating ground arrangement, which allows one to use a single supply voltage and current source, is possible because the CPU prevents more than one electrode pair from being active at any given moment.

The duration of each pulse phase and the intra-pulse interval are typically 20-200 μs. They are timed to 0.16 μs resolution by a 6 MHz timer. Asymmetric amplitude pulses can be created by altering the duration of each pulse to maintain charge balance. A current-to-voltage amplifier in series with the current source relays a measure of actual stimulus current the CPU, through one of the A-D channels of the MSP430.

d. Power – Uninterrupted power is important for this application, because an animal (or person) adapted to tonic stimulation provided by the device could suffer severe vertigo due to acute loss vestibular input in the event of power loss. The device is powered either by a small but high-energy-capacity primary Lithium battery contained within the head-mounted device (e.g., Saft LS14250, 3.6 V, 1000mAh, 14.7mm diam x 24.8mm, 8.9g) or by a rechargeable secondary battery with greater capacity that connects to the device from a body-worn pack (e.g., LENMAR LIJ408, 7.2 V, 1100mAh, 54 x 38 x 22 mm, 71g). This arrangement simplifies replacement of batteries while preventing inadvertent power loss. Unfortunately, the high current draw of the 3 MEMS gyros (~18 mA continuous from a 5V supply generated by a TPS76950 low drop-out regulator) limits battery life to about 48 hours per rechargeable battery.

The MSP430 and other low-level logic devices draw comparatively negligible current from a TPS79730 regulator generating a 3 V supply. An LT1615-1 inductor-based step-up DC-DC converter generates the 24V compliance voltage for electrode stimulator circuitry, which draws negligible mean current due to the low amplitude and duty cycle of pulsatile stimuli.

e. Software – The device includes a JTAG interface for in-circuit programming the flash memory of the MSP430F149 using a laptop computer. This interface also allows one to monitor and change register and RAM values as the device is running *in situ*. We use the Kickstart Embedded Workbench (IAR Systems, Foster City, CA) and FET430 flash emulation tool (Texas Instruments) for program development.

The MSP430F149 remains in a low power mode between interrupts. Interrupts generated by 4 slow timers (clocked by a 32,768 Hz crystal) set the 100 samples/s rate of the A-D converters and the interpulse intervals for each stimulus channel, while interrupts timed by a 6 MHz timer control the duration of the cathodic, intrapulse and anodic phases of each stimulus pulse.

To prevent clashes between multiple channels attempting to enlist the current source simultaneously, the interrupt service routine that normally begins a stimulus pulse first checks to see whether another biphasic pulse is already in progress. In that event, the routine places a request on a queue and exits. At the end of a biphasic stimulus pulse, the program checks this queue and activates a pulse on the next channel in the queue. Given the typical pulse duration of 200 μs/phase and maximum pulse rate of 300 pulse/s on each of 3 channels, the queue is rarely >1 element.

Each input data stream can optionally pass through a digital high pass filter emulating the characteristics of the chinchilla semicircular canals, as described previously by Gong and Merfeld [7].

For each channel, a stimulus interpulse interval ΔT s is computed from the 12-bit ADC output x_i representing head velocity (ADC values of 0, 2048 and 4096 representing head velocity -450, 0 and +450°/s, respectively) by interpolation into a 16 element look up table described by

$$\Delta T = 1/[150 \cdot (1 + \tanh((x_i/1024) - 2.3))] \quad (1)$$

$x_i = 256 \cdot i$ for i = 0-16

which describes a saturating nonlinearity that roughly emulates the spike rate versus head velocity operating curve of regular chinchilla vestibular nerve fibers, upshifted to a resting rate of approximately 100 pulses/s to allow the device to overdrive spontaneous afferent fiber activity and thus provide more dynamic range for encoding inhibitory head rotations.

III. Results

A. Normal Chinchilla 3D Angular Vestibulo-Ocular Reflex

Figure 1 shows all canal-plane components of mean eye velocity for each eye during 1 Hz, 50°/s head rotations of a normal chinchilla in the horizontal, LARP, and RALP directions. Figure 2 shows the gain and phase of the horizontal component of the aVOR during sinusoidal horizontal head rotations, measured in 6 animals at 20-50°/s. These data reveal that the 3D angular vestibulo-ocular reflex of normal chinchillas is like that of forward-eyed animals:

1) Both eyes (black and gray lines in Fig. 1) move with approximately equal speed and direction, about an axis approximately aligned with the axis of head rotation (in the absence of otolith stimulation by tilt or translation).

2) In the absence of vision, the VOR stabilizes the retina (incompletely) with respect to space for head rotations from ~0.2-10 Hz, with aVOR gain (–eye velocity/head velocity) decreasing below 1 Hz (Fig. 2).

3) The aVOR has phase near zero over ~1-10 Hz and has a phase lead below 1 Hz that is typical of a high pass filter with a break frequency at ~0.05-0.1 Hz (Fig. 2).

4) aVOR-mediated eye rotations are symmetric about each rotation axis, with <10% asymmetry noted for responses to nasal and temporal yaw rotations of the head.

These normal characteristics can serve as performance goals for functional electrical stimulation designed to restore the aVOR after bilateral vestibular ablation.

B. 3D Angular Vestibulo-Ocular Reflex Evoked by Functional Electrical Stimulation of the Vestibular Nerve

In otherwise normal chinchillas with all 6 semicircular canals surgically plugged and the otolith sensors surgically disrupted, only minimal (<5°/s RMS) eye movements were observed during 100°/s head rotations in any direction. When sinusoidal head rotation velocity was used to modulate the frequency of pulsatile galvanic stimuli applied via either a monopolar electrode or bipolar pair implanted near the right horizontal semicircular canal's sensory epithelium, the resulting eye movements were similar to normal animals' aVOR responses to horizontal head rotation. Figure 3 shows the horizontal components of left and right eye rotational velocity for one such chinchilla during horizontal head rotation at 1Hz, 20°/s peak, without and with functional electrical stimulation. The stimulus was biphasic, charge-balanced, 175 μA, 200 μs/phase, 200 μs intrapulse interval pulses, modulated over 20-180 pulses/s. Before electrical stimulation begins (Panel A), head rotation elicits no aVOR. When electrical stimulation encoding head velocity begins, horizontal slow phase nystagmus begins, along with saccadic eye movements compensating for slow phase asymmetry. Like the asymmetry observed during sinusoidal head rotation shortly after left labyrinthectomy, this asymmetry stems from imbalance of the mean rate of action potentials on the two vestibular nerves.

Adaptation to unilateral electrical stimulation was remarkably quick. Figure 3, Panel B is a segment of the same trial as Panel A, less than 1 min after onset of stimulation. The slow phase nystagmus is much more symmetric, tracking horizontal head velocity with gain of ~1. The asymmetry is gone, and saccades are rare.

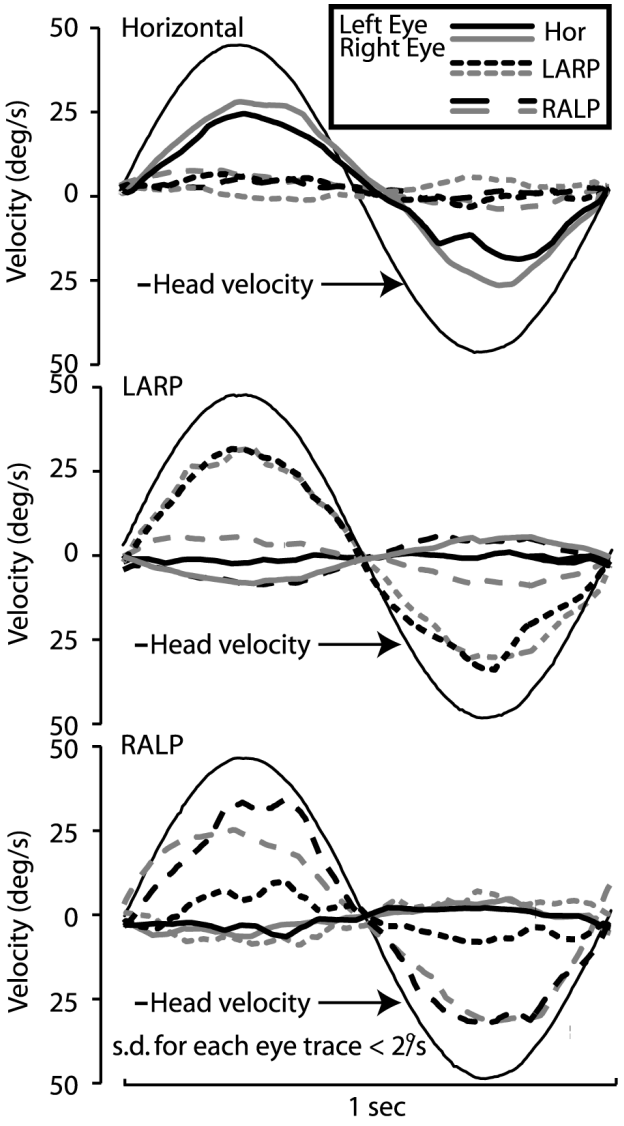

Fig. 1. Mean head rotation and eye rotations of a normal chinchilla during 1 Hz, 50°/s head rotations in dark, in horizontal (top), left-anterior/right-posterior (middle) and right-anterior/left-posterior (bottom) canal planes. Standard deviation of each trace at each time point is < 2°/s.

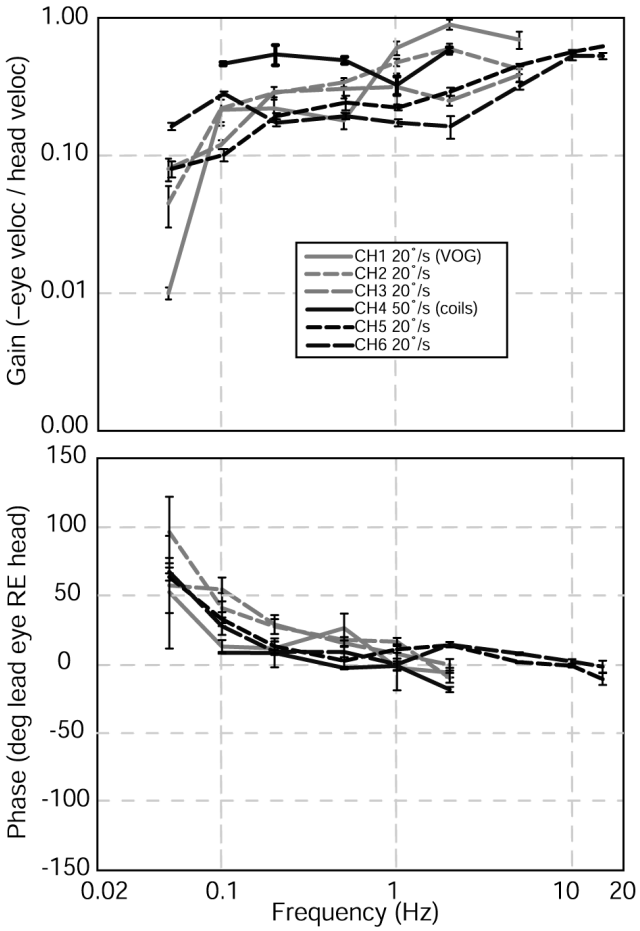

Fig. 2. Gain (top) and phase lead (bottom) of the horizontal component of 3D angular VOR for each of 6 normal chinchillas (one eye each) during 50°/s (animal #4) or 20°/s (all others) head rotation in darkness. Black: measured using scleral search coils. Gray: measured using 3D VOG.

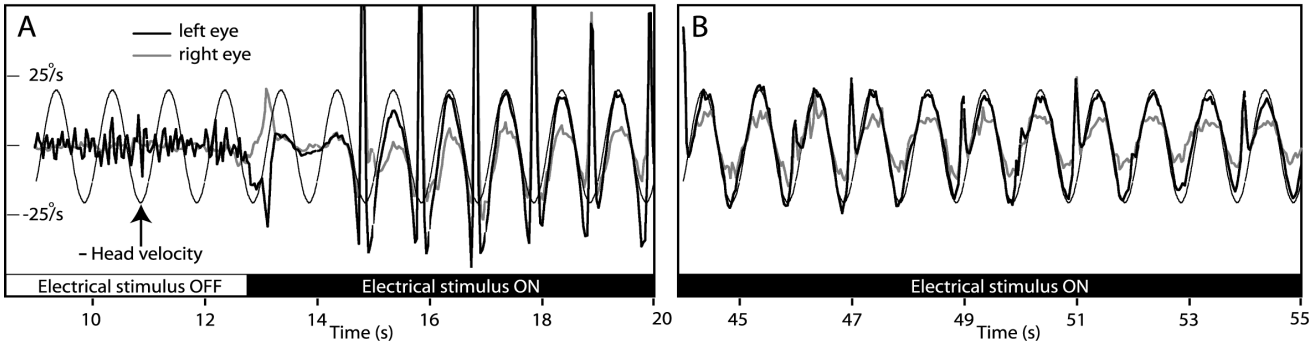

Fig. 3. Horizontal components of head and eye rotational velocity of canal-plugged chinchilla during 1 Hz, 50°/s head rotation about the axis of the horizontal semicircular canal in darkness before (Panel A, white bar), immediately after onset of (Panel A, black bar) and after ~ 1 min of pulse-frequency modulated stimulation via a monopolar electrode in the right horizontal canal ampulla. Head rotation elicits no aVOR without electrical stimulation. Once electrical stimulus begins, an initial slow phase nystagmus asymmetry rapidly adapts to a nearly ideal horizontal aVOR. The decreased right eye response is likely due to lid impact of the fiducial marker used for VOG.

When viewed in only the horizontal dimension, the data of Fig. 3 seem to indicate a nearly perfect horizontal aVOR. However, 3-D oculography during the same trial (Fig. 4) reveals that the evoked eye movements have significant LARP and RALP components, consistent with current spread causing stimulation of the anterior and posterior canal cristae or the otolith endorgans. Subsequent micro-CT imaging of the animal revealed that the electrode was in fact nearly as close to the sensory epithelia of the anterior semicircular canal and utricle as it was to the sensory epithelium of the horizontal canal.

C. Device Testing - 3D Vestibular Prosthesis

Figure 5 shows a photograph of the prosthesis circuitry, and Figure 6 shows the frequency of output pulses on each of three channels configured for biphasic stimulation of the horizontal, anterior and posterior semicircular canals of one vestibular labyrinth. The device was rotated at 2 Hz, 50°/s about each canal's axis. While imperfect alignment of the device with the motor axis led to some crosstalk, the ability of the device to encode 3D head rotations via modulating pulse frequency by canal plane components is apparent.

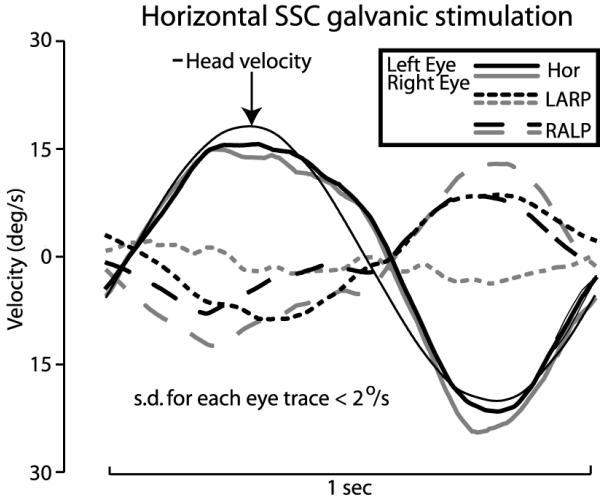

Fig. 4. Same trial as Fig. 3, analyzed in 3D, reveals eye movement components outside the plane of the horizontal canal, evidence of stimulus spread to anterior and posterior canal nerves or otolith endorgans. Mean of 10 cycles, SD < 2°/s for each point of each trace.

IV. Discussion

The 3D angular VOR of normal chinchillas is (partially) compensatory over 0.1-10 Hz, approximately equal for both eyes and symmetric to within ~10%. These findings are consistent with prior studies of rodents and lagomorphs using 1D or 2D eye recordings, except for absence of the large naso-temporal asymmetry that has been described for gerbils [11]-[13]. These results suggest that the chinchilla, despite its lateral eye orientation, is an appropriate animal model for vestibular prosthesis research.

When electrical stimulation responses were analyzed in 1D (as is typical of most small animal aVOR studies), we observed what seemed to be a perfect horizontal aVOR. However, 3-D measurements revealed off-axis components probably due to current spread to other endorgans. Judging from the spectral selectivity achieved by cochlear implants, increased vestibular nerve selectivity should be achievable

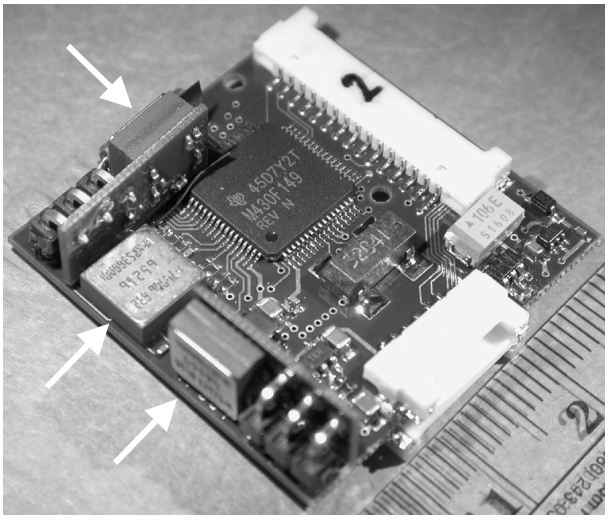

Fig 5. Prosthesis circuitry. Arrows=rotational accelerometers, two of which are on boards perpendicular to the mother board. Scale = cm

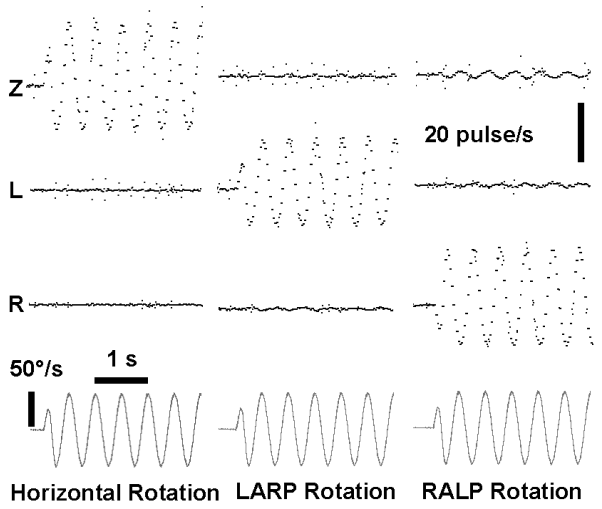

Fig. 6. Pulse rates on each of 3 electrode channels (Z, L, R) encoding components of 3 different 2 Hz, 50 deg/s rotations of the device (bottom) about the horizontal (first column), LARP (second)and RALP(third) axes.

through refinements in electrode design, stimulus protocols and surgical technique. Assaying performance using 3D oculography should facilitate these refinements.

Pulsatile stimuli as used here are exclusively excitatory. For a unilateral vestibular prosthesis to encode head movements in *all* directions (including those that normally *inhibit* canals of the implanted labyrinth), the central nervous system must adapt to a tonic rate of stimulation, above and below which pulse rates encode excitatory and inhibitory head rotations, respectively. Setting the resting rate above the typical resting rate of vestibular nerve afferents can expand the dynamic range for encoding inhibitory head rotations. Lewis, Merfeld and colleagues observed evidence of adaptation over hours to weeks in chronically stimulated guinea pigs and monkeys [8],[14]. They noted that training appeared to increase the speed of adaptation to step changes in tonic stimulus rate. Combined with the rapid resolution of nystagmus asymmetry we observed acutely in chinchillas, these findings suggest that a unilaterally implanted device should be sufficient to restore bi-directional vestibular sensation. This is of practical importance, because the cost and surgical risk of bilateral vestibular implantation would limit clinical utility.

While we have focused on semicircular canals, the otolith endorgans could also be emulated by an electronic device. Adding 3 linear acceleration sensors would only add another ~2 mA to the power use of the device. Unlike the ampullary nerves, the vestibular nerve branches to the otolith endorgans include afferent fibers with a wide range of directional sensitivity, complicating the design of electrodes and stimulus paradigms for otolith endorgans.

Reducing size and power consumption is an important goal for refinement of this device toward clinical application. Smaller rotational sensors with lower power usage, ideally packaged with 3 orthogonal sensors per device, would facilitate further development of vestibular prostheses, as would rechargeable batteries with higher energy density. The 3 gyro sensors collectively draw ~18 mA, accounting for most of the power use. A transcutaneous inductive link for recharging will be a necessity for a fully implantable device designed for human use.

ACKNOWLEDGMENTS

We gratefully acknowledge: Todd Whitehurst, Cliff Brainard and Tom Mehl (Advanced Bionics Corporation), who helped with current source design, board layout and fabrication; Hamish MacDougall (Sydney University), who helped create the VOG system used in this work; Patpong Jiradejvong, Dale Roberts, Paul Gilka and Adrian Lasker (Johns Hopkins), who provided technical assistance with scleral coil recording and soldering; Daniel Merfeld (Jenks Vestibular Laboratory, Massachusetts Eye & Ear Infirmary), whose advice has helped foster this work; and Lloyd Minor (Johns Hopkins Otolaryngology – Head & Neck Surgery), whose mentorship has been integral to the success of this research.

REFERENCES

[1] R.J. Leigh & D.S. Zee *The Neurology of Eye Movements*, 3rd Edition, Oxford University Press,1999.

[2] J.R.Tian, I.Shubayev, J.L.Demer, "Dynamic visual acuity during transient and sinusoidal yaw rotation in normal and unilaterally vestibulopathic humans," *Exp.Brain Res*. Mar 2001;137:12-25.

[3] B.Cohen, J-I Suzuki, M.E.Bender, "Eye movements from semicircular canal stimulation in the cat," *Ann.Otol.Rhinol.Laryngol*. Mar 1964;73:153-169.

[4] K.Ezure, M.S.Cohen, V.J.Wilson, "Response of cat semicircular canal afferents to sinusoidal polarizing currents: implications for input-output properties of second-order neurons," *J Neurophysiol* 1983;49:639-648.

[5] J.M.Goldberg, C.E.Smith, C.Fernandez, "Relation between discharge regularity and responses to externally applied galvanic currents in vestibular nerve afferents of the squirrel monkey,". *J Neurophysiol* Jun 1984;51:1236-1256.

[6] L.B.Minor , J.M.Goldberg, "Vestibular-nerve inputs to the vestibulo-ocular reflex: a functional-ablation study in the squirrel monkey," *J Neurosci* Jun1991;11:1636-1648.

[7] W.Gong and D.M.Merfeld, "Prototype neural semicircular canal prosthesis using patterned electrical stimulation," *Ann.Biomed.Eng* May 2000;28:572-581.

[8] W.Gong and D.M.Merfeld, "System design and performance of a unilateral horizontal semicircular canal prosthesis," *IEEE Trans Biomed Eng* Feb 2002; 49(2), 175-181..

[9] A.A.Migliaccio, H.G.MacDougall, L.B.Minor, C.C.Della Santina, "Inexpensive system for real-time 3-dimensional video-oculography using a fluorescent marker array," *Journal of Neuroscience Methods*, Apr 2005;143(2):141-50

[10] A.A.Migliaccio, M.C.Schubert, P.Jiradejvong, *et al.*, "The three-dimensional vestibulo-ocular reflex evoked by high-acceleration rotations in the squirrel monkey," *Exp Brain Res*. Dec 2004;159(4):433-46.

[11] W.H.Merwin, C.Wall, D.L.Tomko, "The chinchilla's vestibulo-ocular reflex.,"*Acta Otolaryng (Stockh)* Sept 1989; 108:161-7

[12] E.A.Baarsma & H.Collewijn, "Vestibulo-ocular and optokinetic reactions to rotation and their interaction in the rabbit," *J Physiol* May 1974, 238:603-25.

[13] G.Kaufman, "Video-oculography in the gerbil,"*Brain Res* Dec 2002; 958:472-87

[14] R.F.Lewis, W.Gong, M.Ramsey, *et al*.," Vestibular adaptation studied with a prosthetic semicircular canal, " *J Vestib Res*. 2002-2003; 12(2-3):87-94.